03500.018212. PATENT APPLICATION

IN THE UNITED STATES PATENT AND TRADEMARK OFFICE

In re Application of:	)	
	:	Examiner: Ryan A. Lepisto
TOSHIHIKO OUCHI	)	
	:	Group Art Unit: 2883
U.S. Application No.: 10/541,240	)	
	:	
§ 371(c) Date: July 1, 2005	)	
	:	
Int'l Application. No.: PCT/JP2004/004348	)	
	:	
Int'l Filing Date: March 26, 2004	)	
	:	
For: HIGH FREQUENCY ELECTRICAL SIGNAL CONTROL DEVICE AND SENSING SYSTEM	)	
	:	October 8, 2009

Commissioner for Patents
P.O. Box 1450
Alexandria, VA 22313-1450

LETTER SUBMITTING DOCUMENTS FOR PLACEMENT IN FILE

Sir:

Applicant respectfully requests that this letter and the attached documents be placed in the application file.

The document listed below was cited during prosecution of a European patent application related to the above U.S. application. A copy of the document is attached.

LEE et al., "Picosecond-Domain Radiation Pattern Measurement Using Fiber-Coupled Photoconductive Antenna" IEEE Journal on Selected Topics in Quantum Electronics, Vol. 7, No. 4, July/August 2001, pp. 667-673.

In addition, a copy of the European Office Action, which is dated September 18, 2009, is also attached.

No action other than placement in the file is requested.

Applicant's undersigned attorney may be reached in our Costa Mesa, California office at (714) 540-8700. All correspondence should continue to be directed to our below-listed address.

Respectfully submitted,

Attorney for Applicant
Michael K. O'Neill
Registration No.: 32,622

FITZPATRICK, CELLA, HARPER & SCINTO
1290 Avenue of the Americas
New York, New York 10104-3800
Facsimile: (212) 218-2200

FCHS_WS 3923617v1

Picosecond-Domain Radiation Pattern Measurement Using Fiber-Coupled Photoconductive Antenna

Heeseok Lee, Jongjoo Lee, *Student Member, IEEE*, and Joungho Kim, *Member, IEEE*

Abstract—**The photoconductive terahertz measurement technique was used for measurement of the radiation pattern from thick metal slits. Picosecond pulses were generated and detected by an ultrafast optoelectronic technique using a femtosecond pulse laser and a subpicosecond photoconductor. Photoconductive sampling measurements of the polarization-dependent diffraction of the picosecond electromagnetic pulses showed the highly polarized radiation characteristics of the photoconductive probing antenna (PCPA) with the finite-difference time-domain simulation. The radiation patterns from the slits were measured using a fiber-coupled PCPA. Investigation of the spatiotemporal radiation pattern from a thick metal slit shows the usefulness of the present measurement setup for time-domain and broadband antenna characterization. Together with the time-domain radiation pattern, the frequency-domain radiation pattern from the experimental transient response is presented in both amplitude and phase. It is demonstrated that the time-domain radiation pattern measurement using the photoconductive terahertz radiation technique is a promising characterization method for millimeter-wave and submillimeter-wave antenna time-domain testing.**

Index Terms—**Antenna measurement, photoconductive measurement, photoconductive sampling, spatiotemporal radiation pattern, terahertz radiation, time-domain antenna testing.**

I. Introduction

MILLIMETER-WAVE (mm-wave) antennas have attracted considerable attention associated with the development of compact high-performance receivers, transmitters, and imaging arrays for automotive collision avoidance radar and mobile communication systems. Accordingly, for precise and efficient characterization of the required mm-wave antennas, more advanced high-accuracy measurement techniques are needed. So far, most antenna characterization work has been in the area of frequency-domain antenna measurement techniques, even though the antenna time-domain measurement (ATDM) technique has substantial advantages over the frequency domain method. The ATDM technique has inherent merits, including direct time-domain gating and having a simplified measurement setup [1], [2]. Any reflections caused by mismatch, and any unwanted multiple reflections in the antenna's range can be easily removed using the time-domain gating method. Furthermore, any mismatch in the antenna network can be observed distinctively from the measured transient response. This is very helpful for antenna diagnosis [1], [2]. However, the lack of a short electromagnetic pulse generator and picosecond sampling circuitry has restrained the development of the ATDM technique for the mm-wave antenna characterization and testing [3].

The photoconductive sampling technique is used as an ultrafast optoelectronic sampling method for acquiring guided and free-space propagating picosecond electrical pulses [4]–[11]. It is one of the most promising solutions for transient measurements in the picosecond domain. Since photoconductive measurements are inherently synchronized, parasitic reflections in the test environment can be easily removed. Moreover, the picosecond-duration transient response can be acquired with picosecond temporal resolution, using a femtosecond short-pulse laser with less than 100-fs pulse duration and a low-temperature-grown Ga–As (LT-Ga–As) photoconductor with subpicosecond response time. In this paper, the transient radiation pattern from metal (Cu) slits is presented to show the feasibility of the picosecond photoconductive sampling technique for the time-domain characterization of a mm-wave antenna. Using a photoconductive probing antenna (PCPA), transient pulses with less than a 3-ps rise time, and which had more than 70-GHz 3-dB frequency spectrum, were generated and detected. In particular, a radiation pattern from the copper slit was measured using a freely positionable fiber-coupled PCPA. Since the thick-metal slit can be considered as an open-ended parallel-plate waveguide, the presented measurement setup can be said to be useful for mm-wave antenna time-domain characterization. Many applications of photoconductive terahertz radiation and detection have been published [7]–[9]. These have described experiments, where objects were placed between the photoconductive detector and emitter. While these were mainly for spectroscopic purposes [9], there have been few applied to antenna testing. This paper demonstrates how the photoconductive terahertz measurement technique can be used for the time-domain testing of conventional mm-wave antenna. Moreover, this allows a wider range of antenna structures to be investigated than the antennas that are integrally fabricated into the generating structure presented in [8].

First, to show the highly polarized radiation characteristics of the picosecond electromagnetic pulses, using photoconductive measurements, the measured time-domain waveforms and the radiation patterns are investigated by comparing the measured transient response diffracted by metal slits with the theoretical prediction calculated by the finite-difference time-domain (FDTD) method [12].

Manuscript received January 8, 2001; revised July 9, 2001. This work was supported by KOSEF under the ERC program through the MINT Research Center, Dongguk University, Seoul, Korea. H. Lee was supported by the Korea Foundation for Advanced Studies (KFAS).

The authors are with Terahertz Media and System Laboratory, Department of Electrical Engineering and Computer Science, Korea Advanced Institute of Science and Technology, Yusong, Taejon 305-701, Korea (e-mail: heeslee@ee-info.kaist.ac.kr).

Publisher Item Identifier S 1077-260X(01)09952-X.

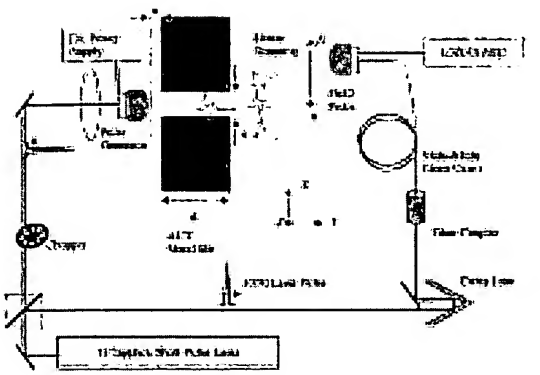

(a)

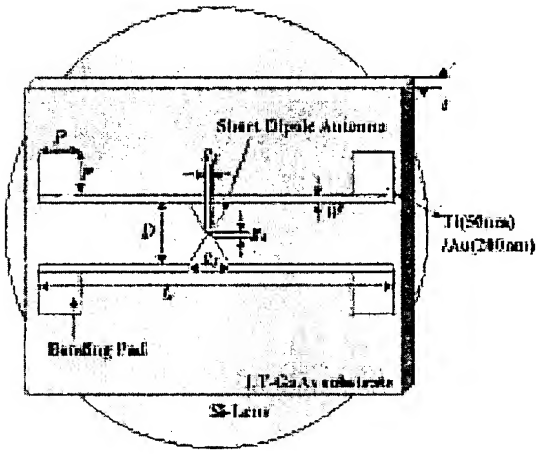

(b)

Fig. 1. (a) Schematic of the photoconductive measurement system for radiation pattern measurement. The distance between the PCPG and the PCPA is 4 cm. The spacing (c) between the PCPG and the slits is less than 0.5 mm. (b) Schematic of the photoconductive antenna for the PCPG and the PCPA fabricated on an LT-Ga–As substrate attached to a hemispherical Si-lens. The thickness (t) of the LT-Ga–As substrate is about 600 μm, and $D = 1500\,\mu$m. The size of the photoconductive gap: $(g_1) = 5\,\mu$m; $g_2 = 20\,\mu$m; $g_3 = 1500\,\mu$m; $L = 10$ mm; and $W = 40\,\mu$m. The pad size is 1 mm^2 ($P \times P$). The diameter of the hemispherical Si-lens is 12 mm.

II. Fiber-Coupled Photoconductive Antenna Setup

The fiber-coupled PCPA system setup is illustrated in Fig. 1(a). The measurement setup consists of a photoconductive pulse generator (PCPG), a PCPA, a femtosecond short pulse laser, an optical delay, and a data acquisition system. The conventional photoconductive antenna, which is used for both the PCPG and the PCPA, has a photoconductive switch coupled with a short dipole antenna structure. The photoconductive antenna is designed to launch and detect terahertz radiation and is deposited on an LT-Ga–As epitaxial layer. The LT-Ga–As layer was grown by molecular beam epitaxy at 200 °C and annealed at 600 °C for 10 min to ensure a subpicosecond carrier lifetime [13]. The detailed structure of the photoconductive antenna is shown in Fig. 1(b). A hemispherical Si-lens is attached to both the PCPG and the PCPA for impedance matching between the Ga–As substrate and free space. To demonstrate the highly polarized radiation from the photoconductive antenna, thick-metal slits were located at a fixed position between the PCPG and the PCPA. In the next section, the properties are discussed with the theoretical verification. On placing 10-mm thick 4-mm wide copper slits between the PCPG and the PCPA, the spatiotemporal radiation patterns were measured; this is discussed in the following section.

A mode-locked Ti–sapphire laser operating at 820 nm with a repetition rate of 76 MHz produced 100-fs duration pulses that were split into two beams, with one variably delayed with respect to the other. The first optical short pulse, modulated by a mechanical chopper at 2 kHz, was focused onto the photoconductive switch of the pulse generator biased at 40 V for the picosecond pulse generation. The second optical pulse was coupled into a 50-cm-long multimode fiber (MMF) to activate the photoconductive switch of the PCPA. We found that the temporal waveform measured with the 50-cm MMF was same as the transient waveform measured without the MMF. Since the dispersion of the short laser pulse propagating through the MMF was less than 1 ps, the effect of the MMF on the transient response of the PCPA was considered to be negligible. The output of the fiber-coupled PCPA was connected to a lock-in amplifier whose amplified output was connected to the data acquisition system.

By moving the position of the fiber-coupled PCPA, the spatiotemporal radiation pattern could be obtained as a function of position [X in Fig. 1(a)]. The polarization of the picosecond electromagnetic pulse generated by the pulse generator could be determined from the orientation of the photoconductive antenna. The direction of the generated electric field from the pulse generator is parallel to the direction of the dipole antenna in the PCPG. The distance between the PCPG and the PCPA was 4 cm, and the spacing (c) between the PCPG and the slits was less than 0.5 mm. In the experimental measurement of spatiotemporal radiation pattern, since the PCPG and the slit were tightly coupled, the diffraction of the terahertz beam radiated by the PCPG at the slit coupling was not considered to be a significant problem. Linear scanning measurements were made at every position along the X direction, in spacings of 0.5 mm on a vertical-probing track, as shown in Fig. 1(a).

III. Highly Polarized Radiation

To exhibit the highly polarized electromagnetic radiation from the photoconductive antenna, the transient waveforms diffracted from the metal (Cu) slits were measured using the photoconductive apparatus at $X = 0$ in Fig. 1(a) and numerically calculated using the FDTD method. In this experiment, since a 6-cm-diameter off-axis parabolic reflector between the PCPG and the metal slits was used to collimate the terahertz beam, the metallic slits were illuminated by the terahertz beam under the far field condition. In Fig. 2, the measured and the calculated results are given by the solid line and the dotted line, respectively. In the FDTD simulation, the incident waveform on the metallic slits was assumed to be the same as the waveform measured without slits, and a perfect electric conductor was used for the slits in the FDTD simulation. The temporal profiles of the TM-polarized pulses scattered through a 4-mm wide slit were very similar to the waveforms measured without a slit. For both 0.25-mm and 10-mm-thick metal slits, the profile of the original waveform was maintained. However, the temporal profiles of the TE-polarized pulse scattered through a

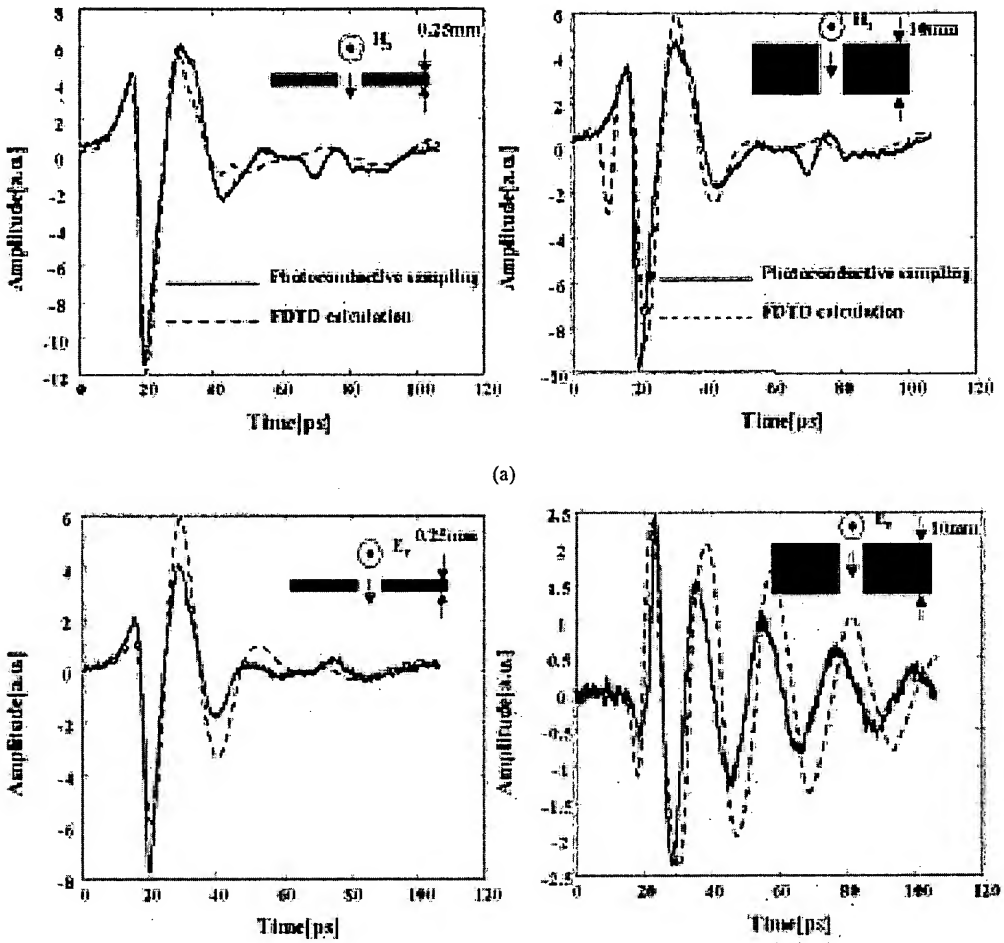

Fig. 2. Polarization-dependent diffraction of the picosecond pulse by the slits. The solid lines indicate the waveform measured by the PCPA, and the dotted lines represent the calculated waveform of the FDTD. For (a), the incident pulse is TM-polarized. For (b), the incident pulse is TE-polarized. In left ones, a 0.25-mm thick 4-mm-wide metal slit was used. In right ones, a 10-mm thick 4-mm wide metal slit was used.

4-mm-wide slit were distorted. In particular, the TE-polarized pulse propagating through a 4-mm-wide and 10-mm-thick slit showed oscillation.

Theoretically, the polarization-dependent diffraction can be explained by considering the boundary conditions in the electromagnetic scattering problem and using waveguide mode theory. Inside the slit, the electric field of the TE-polarized pulse must satisfy Dirichlet's condition, and the magnetic field of the TM-polarized pulse should fit Neumann's condition. In the slit, the TE-polarized field should be expanded as a sine series, and the TM-polarized field should be expanded by cosine series. Hence, the dominant mode of the scattered field in the TM-polarized pulse is a uniform field (m = 0, TM_0) across the slit, whose temporal profile is not affected by the presence of the slit. This means that the propagation of the TM-polarized pulse can support a TEM-mode through the slits. However, the dominant mode of the scattered field in the TE-polarized pulse has a sinusoidal profile across the slit (m = 1, TE_1). This results in a change of the temporal profile of the scattered picosecond pulse. In the case of the TE-polarized pulse given in Fig. 2(b), the phase-front passing through the metal slit is constructed from the multiple reflections occurring inside the slit. In other words, the wavevector (k) of the dominant propagation mode of the TM-polarized pulse is parallel to the y-axis (in Fig. 1). However, there is no propagation mode of the TE-polarized pulse with its wavevector parallel to y-axis. Therefore, when the TE-polarized pulse is incident to a metal slit, the slit can be considered to be a cavity (or a band rejection filter), which is easily observed in Fig. 2(b). The oscillating frequencies correspond to the harmonics of the first resonant frequency at the metallic slit. The lowest resonant frequency can be found at the fourth oscillation of the transient waveform given in the right side of Fig. 2(b). In this figure, the oscillating period is about 25 ps, and it corresponds to the response of the 3.7–mm-wide metal slit. The discrepancy between the measured and the calculated waveform is considered to be due to the disagreement between the designed and the fabricated width of the metal slit. The late time responses shown in Fig. 2(a)–(c) are found at same period around 70 ps, which appeared at 50 ps after the main peak. Although the terahertz beam reflected at a parabolic reflector is known to be collimated, the terahertz ray is scattered at the edge of the parabolic reflector. The distance between the metal slit and the edge of the parabolic reflector was 2 cm. Since the center of the reflector was aligned to the center of the metal slit, the additional flight length (l) is obtained by $(2+l)^2 = 2^2+3^2$. Since l is about 1.6 cm, the late time response is believed to be

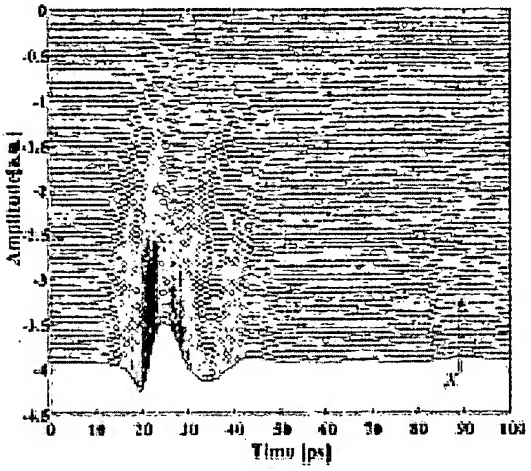

(a)

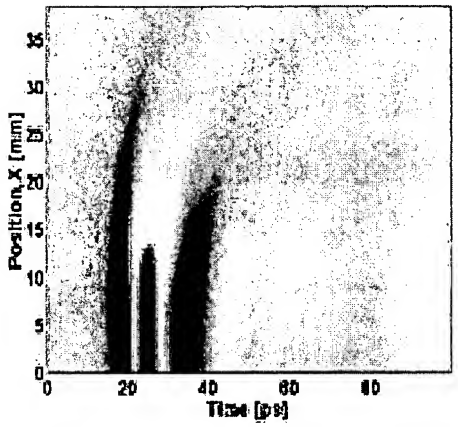

(b)

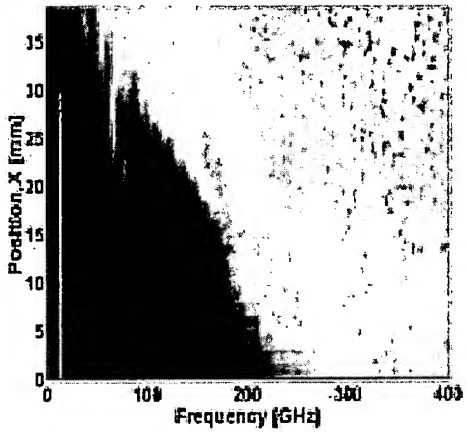

(c)

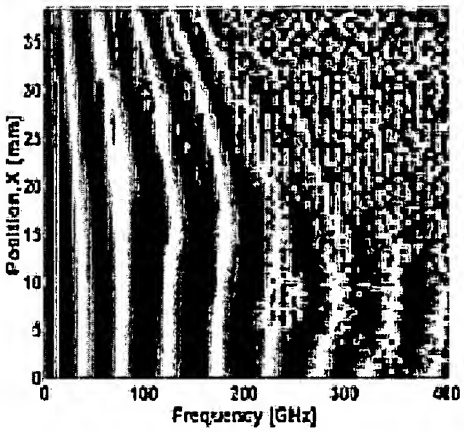

(d)

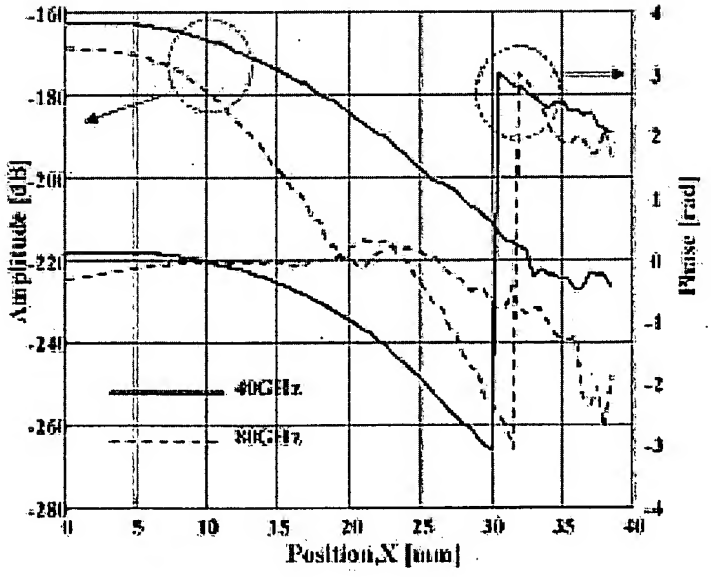

(e)

Fig. 3. Radiation patterns with no slit. (a) and (b) show the spatiotemporal radiation pattern. (c)–(f) show the frequency-domain radiation patterns in amplitude and phase. (c) and (d) are the amplitude and the phase of the frequency-domain radiation pattern, respectively. (e) shows the amplitude and phase pattern at 40 and 80 GHz.

caused by the scattering at the edge of the parabolic reflector. Because 1.6 cm corresponds to 53.3 ps, in Fig. 2(d), this late time response was hidden by the strong oscillation of the transient response. While the parabolic metallic reflector was used in the experimental measurement, the incident wave was assumed to be a plane wave without the parabolic reflector in

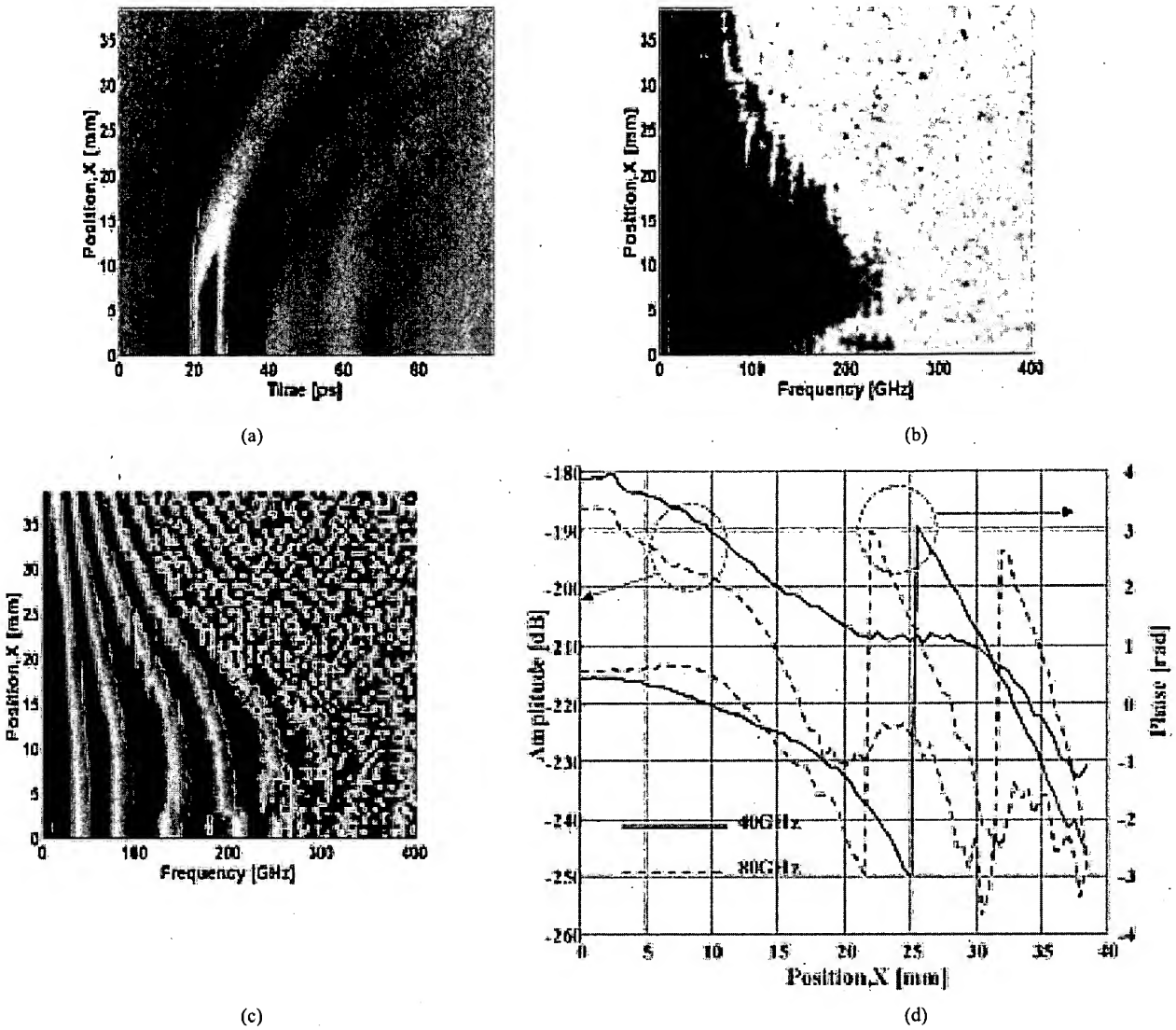

Fig. 4. Radiation pattern using the 10-mm-thick 4-mm-wide TM-polarized metal-slit. (a) Spatiotemporal radiation patterns. (b)–(d) Frequency-domain radiation patterns in amplitude and phase. (b) and (c) are the amplitude and the phase of the frequency-domain radiation patterns, respectively. (d) Amplitude and the phase patterns at 40 and 80 GHz. The linear scanning was performed perpendicular to the slit.

FDTD simulation. Therefore, there is no late-time response in the waveform calculated by FDTD simulation. The tendency of the scattering shown by the FDTD simulation agrees well with that of the measured waveforms and the theoretical prediction, implying that the highly polarized radiation characteristics of the photoconductive electromagnetic pulse generation have been successfully demonstrated. In addition, the close agreement between the measured and the calculated results confirms the fact that the polarization of the PCPG can be easily determined.

IV. Spatiotemporal Radiation Pattern Measurements

The radiation pattern shown in Fig. 3 was measured with no slit. Therefore, the spatiotemporal radiation pattern presented in Fig. 3 is that of the PCPG. The radiation patterns given in Figs. 4 and 5 were measured by placing the 10-mm-thick 4-mm-wide copper slit between the PCPG and the PCPA. In Figs. 4 and 5, the metal slit was oriented parallel to the magnetic field of the radiated pulse from the PCPG (TM-polarized metal slit) and parallel to the electric-field (TE-polarized metal slit), respectively. When the slit was placed in the TE-polarized orientation, the linear scanning was performed along the slit. The polarization of the incident pulse was easily changed by simply rotating the slit. Part (a) of Figs. 3–5 show the measured spatiotemporal radiation patterns. From Figs. 3(b), 4(a), and 5(a), the peak position of the measured waveform is delayed as the probing position is moved away from the center of the slit. This is caused by the following condition: because the radiation patterns are detected by linear scanning, the distance from the radiation source is varied for each scanning position X. In addition, it can be observed that the pulse is broadened as the probing position is moved away from the center of the aperture. This leads to the conclusion that the high-frequency radiation is diminishing as the radiation angle is increasing.

Since the frequency-domain radiation pattern is more conventional for classic antenna engineering, The Fourier transforms

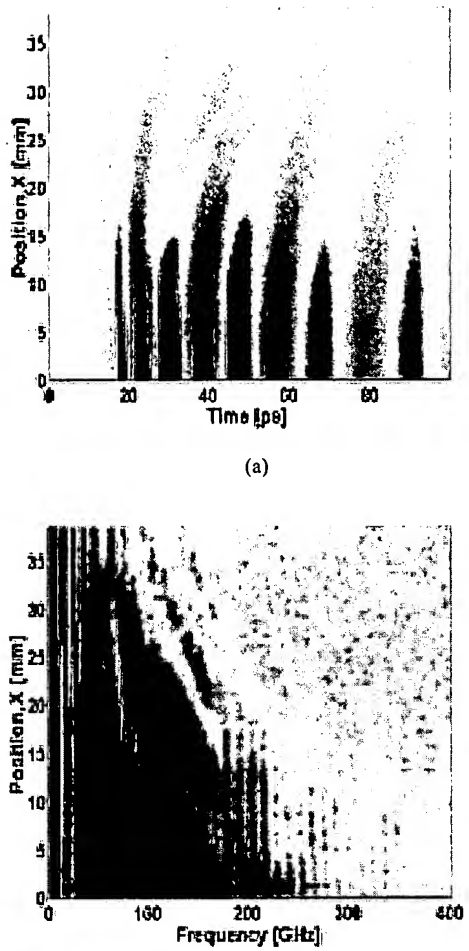

Fig. 5. Radiation pattern with the 10-mm-thick 4-mm-wide TE-polarized metal slit. (a) Spatiotemporal radiation patterns. (b) Frequency-domain radiation patterns in amplitude. The linear scanning was performed parallel to the slit.

of the spatiotemporal radiation patterns are presented from the spatiotemporal radiation patterns. In Fig. 4(b) and (c), the broadband radiation patterns are presented up to a few hundred gigahertz. As shown in Fig. 4(d), the single-frequency radiation patterns in amplitude and phase are taken from Fig. 4(b) and (c) at 40 and 80 GHz, in which the solid line indicates the 40-GHz radiation pattern, and the dotted line represents the radiation pattern at 80 GHz. Figs. 3(c), 4(b), and 5(b) remind us that the high-frequency radiation is diminishing as the radiation angle is increasing.

The broadband radiation patterns are shown. While the amplitude information over 100 GHz is not accurate owing to the frequency spectrum limit, the phase information given by Figs. 3(d) and 4(c) is distinct, even at frequencies above 200 GHz. The equiphase curves in Figs. 3(d) and 4(c) are more curved with increasing frequency. Since the phase term in the frequency domain is the product of the wavenumber proportional to the frequency and the distance (r) from the radiation source, the phase increases as r increases. As previously explained, because the scanning was performed by movement of a linear stage, r increases as X increases. As shown in Fig. 4(d), the slope of the phase at 80 GHz is larger than that at 40 GHz. Comparing Figs. 3(d) and 4(c), the equiphase curves in Fig. 4 are more bent. In the experimental situation of Figs. 3 and 4, r is effectively about 4 and 3 cm, respectively, at $X = 0$. Therefore, the increment of r with respect to the increment of X in the case of Fig. 4 is larger than that in the case of Fig. 3. From Fig. 5, the band-rejected pulse by the TE-polarized metal slit is observed. In this case, r must be same as that in the case of Fig. 3(d). While the TM-polarized slit regenerates the equiphase plane of the radiated pulse at the aperture of the metallic slit, the TE-polarized metal slit simply acts as a band-stop filter.

In this case, since the secondary radiating structure of the thick metallic slit is placed at the near-field region of the primary radiation source of the PCPG, strictly speaking, the radiation pattern presented in Fig. 4 is not the diffraction pattern of the metallic slit with incident plane wave. Since the 10-mm-thick 4-mm-wide slit used in this experiment can be considered as a secondary radiating structure, the radiation pattern shown in Fig. 4 is the E-plane radiation pattern of the 4-mm-wide aperture open-ended parallel-plate waveguide antenna tightly coupled by the PCPG.

Consequently, the feasibility of the presented measurement for time-domain characterization of the mm-wave antenna is shown. Moreover, commercially available mm-wave antenna systems consist of two antenna structures. One is the feed antenna, which is usually a dipole or loop antenna, and the other is a secondary radiating structure to improve the radiation pattern. Mostly, the secondary antenna is placed in the near-field region of the feeding antenna. Therefore, the presented PCPG can be considered as a feed antenna, whose frequency spectrum covers the mm-wave region, and thus the characterization of a radiating structure (secondary antenna) fed by the PCPG can be easily performed using the present measurement setup. This allows a wider range of antenna structures to be investigated than the antennas that are integrally fabricated into the generating structure described in [8].

The radiation pattern measured by the PCPA corresponds to the convolution product of the radiated pattern of the radiating structure and the response of PCPA. Because the probe used in the present experiments includes the 0.6-mm Ga–As substrate and a high index material such as a silicon lens, the measured radiation pattern is perturbed. To minimize the effect from the response of the probe antenna, a micro-machined photoconductive probe recently developed by the authors [15], or the electrooptic sensors presented in [16]–[18], can be used in replacement of the present PCPA.

V. Conclusion

The radiation patterns from metal slits were measured using a fiber-coupled PCPA. The overall agreement between the measured results and the theoretical predictions by FDTD simulation present a convincing demonstration of its highly polarized radiation properties and of the usefulness of the photoconductive sampling method for time-domain mm-wave antenna testing. It demonstrates the practical use of the picosecond photoconductive sampling technique for the time-domain charac-

terization of mm-wave antennas. In particular, the present measurement technique will be very useful for broadband antenna time-domain characterization. The recent introduction of compact short pulse fiber lasers [14] means that the measurement setup can be built on a small table, showing the high potential and usefulness of the present photoconductive sampling technique for practical time-domain antenna tests.

REFERENCES

[1] R. V. de Jongh, M. Hajian, and L. P. Lighart, "Antenna time-domain measurement techniques," *IEEE Antennas Propagat. Mag.*, vol. 39, pp. 7–11, Oct. 1997.

[2] O. E. Allen, D. A. Hill, and A. R. Ondrejka, "Time-domain antennas characterization," *IEEE Trans. Electromagn. Compat.*, vol. 35, pp. 339–345, 1993.

[3] N. S. Nahman, "Picosecond-domain waveform measurements: Status and future directions," *IEEE Trans. Instrum. Meas.*, vol. IM-32, pp. 117–124, Mar. 1983.

[4] J. Kim, S. Williamson, J. Nees, S. Wakana, and J. F. Whitaker, "Photoconductive sampling probe with 2.3 ps temporal resolution and 4 μV sensitivity," *Appl. Phys. Lett.*, vol. 62, pp. 2268–2270, May 1993.

[5] T. Pfeifer, H.-M. Heiliger, H. G. Roskos, and H. Kurz, "Generation and detection of picosecond electric pulses with freely positionable photoconductive probes," *IEEE Trans. Microwave Theory Technol.*, vol. 43, pp. 2856–2862, Dec. 1995.

[6] P. R. Smith, D. H. Auston, and M. C. Nuss, "Subpicosecond photoconducting dipole antennas," *IEEE J. Quantum Electron.*, vol. QE-24, pp. 255–260, Feb. 1988.

[7] K. Agi and L. Carin, "Ultra-wideband three-dimensional scattering using optoelectronically switched antennas," in *IEEE Antennas Propagat. Soc. Int. Symp. 1992*, vol. 2, pp. 662–665.

[8] Y. Pastol, G. Arjavalingam, and J.-M. Halbout, "Characterization of an optoelectronically pulsed equiangular spiral antenna," *Electron. Lett.*, vol. 26, pp. 133–135, Jan. 1990.

[9] D. R. Grischkowsky, S. Keiding, M. Exter, and Ch. Fattinger, "Far-infrared time-domain spectroscopy with terahertz beams of dielectrics and semiconductors," *J. Opt. Soc. Am. B.*, vol. 7, pp. 2006–2015, Oct. 1990.

[10] P. Uhd Jepsen, R. H. Jacobseb, and S. R. Keiding, "Generation and detection of terahertz pulses from biased semiconductor antennas," *J. Opt. Soc. Amer.*, vol. B13, pp. 2424–2436, 1996.

[11] O. Mitrofanov, I. Brener, M. C. Wanke, R. R. Ruel, J. D. Wynn, A. J. Bruce, and J. Federici, "Near-field microscope probe for far infrared time domain measurements," *Appl. Phys. Lett.*, vol. 77, pp. 591–593, July 2000.

[12] A. Taflove, *Computational Electrodynamics: The Finite-Difference Time-Domain Method.* New York: Artech, 1995.

[13] S. Gupta, J. F. Whitaker, and G. A. Mourou, "Ultrafast carrier dynamics in III–V semiconductors grown by molecular-beam epitaxy at very low substrate temperatures," *IEEE J. Quantum. Electron.*, vol. 28, pp. 2464–2472, Oct. 1992.

[14] E. P. Ippen and H. A. Haus, "Short-pulse fiber lasers," in *IEEE Lasers Electro-Optics Soc. Annu. Meeting*, vol. 2, 1996, p. 379.

[15] J. Lee, H. Lee, and J. Kim, "Micromachined photoconductive electric field mapping probe for the measurement of picosecond pulse propagation," in *2000 IEEE LEOS Annu. Meeting*, vol. 1, 2000, pp. 41–42.

[16] K. Yang, G. David, J. G. Yook, I. Papapolymerou, L. P. B. Katehi, and J. F. Whitaker, "Electrooptic mapping and finite-element modeling of the near-field pattern of a microstrip patch antenna," *IEEE Trans. Microwave Theory Technol.*, vol. 48, pp. 288–294, Feb. 2000.

[17] K. Yang, L. P. B. Katehi, and J. F. Whitaker, "Electro-optic field mapping system utilizing external gallium arsenide probes," *Appl. Phys. Lett.*, vol. 77, pp. 486–488, July 2000.

[18] S. G. Park, M. R. Melloch, and A. M. Weiner, "Analysis of THz waveforms measured by photoconductive and electrooptic sampling," *IEEE J. Quantum Electron.*, vol. 35, pp. 810–819, 1999.

Heeseok Lee was born in Seoul, Korea, in October 1973. He received the B.S. degree in electronic communication engineering from Hanyang University, Seoul, in 1996 and the M.S. degree from Korea Advanced Institute of Science and Technology (KAIST), Taejon, Korea, where he is currently pursuing the Ph.D. degree.

Since then, he has been with the Terahertz Media and System Laboratory in electrical engineering, KAIST, where he is involved with terahertz imaging using photoconductive sampling and FDTD modeling of the high-speed digital interconnection. His current research interests are signal integrity, EMI/EMC, and computational electromagnetics such as FDTD. He was a scholarship student supported by the Korea Foundation for Advanced Studies.

Jongjoo Lee (S'99) received the B.S. degree in electronics from Kyungpook National University, Taegu, Korea, in 1994 and the M.S. degree in electrical engineering from Korea Advanced Institute of Science and Technology (KAIST), Taejon, Korea, where he is currently pursuing the Ph.D. degree.

He was involved in MMIC and OEIC design and semiconductor microfabrication. In 1997, he joined the Terahertz Media and System Laboratory in electrical engineering, KAIST. His doctoral work is on the development of a picosecond electric near-field mapping technique based on photoconductive sampling and the application of the technique to the characterization of picosecond electric signal propagation phenomena. He has been supported as a scholarship student of the Korea Research Foundation under Grants for the Junior Researchers Program.

Joungho Kim (S'89–M'93) received the B.S. and M.S. degrees from Seoul National University, Seoul, Korea, in 1984 and 1986, respectively, and the Ph.D. degree from the University of Michigan, Ann Arbor, in 1993, all in electrical engineering.

His doctoral research was the development of femtosecond time-domain optical measurement techniques for the testing of high-speed digital devices and millimeter-wave circuits. He joined Picometrix, Inc., Ann Arbor, in 1993 as a Research Engineer, where he was responsible for the development of a picosecond sampling system and a 70-GHz photoreceiver. In 1994, he joined the Memory Division of Samsung Electronics, Kiheung, Korea, where he was engaged in a 1-Gbit DRAM design. In 1996, he joined the Korea Advanced Institute of Science and Technology (KAIST), Taejon, Korea. He is currently an Associate Professor in the Electrical Engineering and Computer Science Department. Since joining KAIST, his research interests have centered on high-speed interconnection and package. He teaches a course in high-speed interconnection and packages at the graduate level. His research topics include high-speed package modeling, on-chip interconnection modeling, crosstalk modeling, and low SSN power/ground design. In addition, he has conducted research on EMI/EMC problems of high-speed devices, interconnection, and systems. Also, he has developed a novel picosecond/terahertz near-field imaging system for the high-frequency characterization of interconnections. He is now on sabbatical leave during the academic year 2001–2002 at Silicon Image Inc., Sunnyvale CA, as a Staff Engineer. He has authored or coauthored more than 100 technical articles and numerous patents.

Europäisches Patentamt
European Patent Office
Office européen des brevets

European Patent Office
Postbus 5818
2280 HV Rijswijk
NETHERLANDS
Tel: +31 70 340 2040
Fax: +31 70 340 3016

TBK-Patent
Bavariaring 4-6
80336 München
ALLEMAGNE

RECEIVED
EINGEGANGEN
23. Sep. 2009
TBK PATENT

Formalities Officer
Name: Walsh, Eric
Tel: +31 70 340 - 0
or call
+31 (0)70 340 45 00

Substantive Examiner
Name: Pastor Jiménez, J
Tel: +31 70 340 - 4965

Application No.	Ref.	Date
07 150 006.0 - 1248	EP53452	18.09.2009
Applicant: CANON KABUSHIKI KAISHA		

Communication pursuant to Article 94(3) EPC

The examination of the above-identified application has revealed that it does not meet the requirements of the European Patent Convention for the reasons enclosed herewith. If the deficiencies indicated are not rectified the application may be refused pursuant to Article 97(2) EPC.

You are invited to file your observations and insofar as the deficiencies are such as to be rectifiable, to correct the indicated deficiencies within a period

of 4 months

from the notification of this communication, this period being computed in accordance with Rules 126(2) and 131(2) and (4) EPC. One set of amendments to the description, claims and drawings is to be filed within the said period on separate sheets (R. 50(1) EPC).

Failure to comply with this invitation in due time will result in the application being deemed to be withdrawn (Art. 94(4) EPC).

Europäisches Patentamt • European Patent Office • Office européen des brevets

Frist : 28.1.10 ✓ nicht verlängerbar
Term: not extendible

W 18.10.09 ✓

Pastor Jiménez, J
Primary Examiner
For the Examining Division

Enclosure(s): 3 page/s reasons (Form 2906)
xp1106l969

The examination is being carried out on the **following application documents**:

Description, Pages

1-42 as originally filed

Claims, Numbers

2-8 as originally filed

1 received on 03.07.2008 with letter of 03.07.2008

Drawings, Sheets

1/14-14/14 as originally filed

1. Reference is made to the following documents; the numbering will be adhered to in the rest of the procedure:

   D1: EP-A-0 354 308 (IBM [US]) 14 February 1990 (1990-02-14)
   D2: GB-A-2 371 618 (TERAPROBE LTD [GB]; TERAVIEW LTD [GB]) 31 July 2002 (2002-07-31)

   The following document D3 is cited by the Examiner found in a further search (see Guidelines C-VI, 8.2 and 8.3). A copy of the document is annexed to the communication and the numbering will be adhered to in the rest of the procedure:

   D3: XP 11061969 "Picosecond-domain radiation pattern measurement using fiber-coupled photoconductive antenna" Heeseok Leek et al. IEEE Journal on selected topics in quantum electronics, vol. 7, N° 4, July/August 2001.

2. The application does not meet the requirements of Article 84 EPC, because claim 1 is not clear.

   Claim 1 does not meet the requirements of Article 84 EPC in that the matter for which protection is sought is not defined. The claim attempts to define the subject-matter in terms of the result to be achieved ("for performing switching between a first state where an electromagnetic wave output from the transmitter is input directly into the receiver through the transmission line without being radiated to the space via the antenna and a second state where an electromagnetic wave output from the transmitter to the transmission line is radiated via the antenna and an electromagnetic wave in the frequency band is received by the antenna and the received electromagnetic wave is input into the receiver through the transmission line"). Such a definition is only allowable under the conditions

elaborated in the Guidelines C-III, 4.10. In this instance, however, such a formulation is not allowable because it appears possible to define the subject-matter in more concrete terms, viz. in terms of how the effect is to be achieved.

3. The present application does not meet the requirements of Article 52(1) EPC because the subject-matter of claims 1, 4, 5, 7 and 8 is not new within the meaning of Article 54(1) and (2) EPC.

3.1. Document D3 discloses (the references in parentheses applying to this document):
An electromagnetic wave control device (abstract), comprising as arranged on a substrate (figure 1(b)):
a transmitter (page 668, left-column, lines 8-10) for outputting an electromagnetic wave of a frequency band ranging from 30 GHZ to 30 THZ (abstract);
a transmission line (figure 1 (b)) for propagating the electromagnetic wave of the frequency band output from the transmitter;
a receiver (page 668, left-column, lines 8-10) for receiving an electromagnetic wave of the frequency band through the transmission line; and
an antenna (figure 1(b), "Short dipole antenna") for radiating the electromagnetic wave output from the transmitter and propagated through the transmission line to the space or receiving the electromagnetic wave of the frequency band to be input into the receiver through the transmission line (figures 1, 2),
the device further comprises a switch (page 668, left-column, lines 5-8) for performing switching between a first state where an electromagnetic wave output from the transmitter is input directly into the receiver through the transmission line without being radiated to the space via the antenna and a second state where an electromagnetic wave output from the transmitter to the transmission line is radiated via the antenna and an electromagnetic wave in the frequency band is received by the antenna and the received electromagnetic wave is input into the receiver through the transmission line.

The subject-matter of claim 1 is therefore not new (Article 54(1) and (2) EPC).

3.2. Document D3, figure 1(b) discloses the additional features of dependent claims 4, 5 and 8.
Document D1, abstract discloses the additional features of dependent claim 7.

4. The present application does not meet the requirements of Article 52(1) EPC because the subject-matter of claims 2, 3 and 6 does not involve an inventive step within the meaning of Article 56 EPC.

According to what is disclosed in document D3, the person skilled in the art would consider as obvious the additional features of dependent claim 2, providing no surprising effect and rendering the subject-matter of such claim not inventive.

The additional features of dependent claims 3 and 6 are merely one of several straightforward possibilities which the skilled person would select, depending on the circumstances, without exercising inventive skill.

5. In the event of a continuation of the procedure, the applicant is invited to take account of the following:

5.1. To meet the requirements of Rule 42(1)(b) EPC, the documents D1-D3 should be identified in the description and the relevant background art disclosed therein should be briefly discussed.

5.2. To meet the requirements of Rule 43(1) the independent claims should be properly recast in the two-part form.

5.3. The features of the claims should be provided with reference signs placed in parentheses to increase the intelligibility of the claims (Rule 43(7) EPC). This applies to both the preamble and characterising portion (see the Guidelines, C-III, 4.19).

5.4. In order to facilitate the examination of the conformity of the amended application with the requirements of Article 123(2) EPC, the applicant is requested to clearly identify the amendments carried out, irrespective of whether they concern amendments by addition, replacement or deletion, and to indicate the passages of the application as filed on which these amendments are based.

If the applicant regards it as appropriate these indications could be submitted in handwritten form on a copy of the relevant parts of the application as filed.